Research Article Vol. 2, No. 2 / February 2015 / Optica 162

Measuring the absorption coefficient of biological materials using integrating cavity ring-down spectroscopy

Michael T. Cone,[1] John D. Mason,[1] Eleonora Figueroa,[1] Brett H. Hokr,[1,2,3] Joel N. Bixler,[2,4] Cherry C. Castellanos,[3] Gary D. Noojin,[3] Jeffrey C. Wigle,[4] Benjamin A. Rockwell,[4] Vladislav V. Yakovlev,[1,2] and Edward S. Fry[1,*]

[1]Department of Physics & Astronomy, Texas A&M University, College Station, Texas 77843, USA

[2]Department of Biomedical Engineering, Texas A&M University, College Station, Texas 77843, USA

[3]TASC Inc., San Antonio, Texas 78228, USA

[4]711th Human Performance Wing, Human Effectiveness Directorate, Bioeffects Division, Optical Radiation Bioeffects Branch, JBSA Fort Sam Houston, Texas 78234, USA

*Corresponding author: fry@physics.tamu.edu

Received 24 September 2014; revised 20 December 2014; accepted 22 December 2014 (Doc. ID 223768); published 16 February 2015

A number of imaging modalities rely on the exact knowledge of both the absorption and scattering properties of cells and organelles. We report a simple method for accurate and precise measurement of the optical absorption coefficient of biological samples, even in the presence of strong scattering. The technique is based on cavity ring-down spectroscopy, but the traditional mirrored cavity is replaced with a high-reflectivity integrating cavity. The Lambertian behavior of the cavity walls creates an isotropic field inside the cavity, thereby eliminating the effects of scattering in the sample. Thus, integrating cavity ring-down spectroscopy (ICRDS) provides a true, direct measurement of the absorption coefficient, as opposed to the net attenuation. We demonstrate the effectiveness of this technique by measuring the absorption coefficient of retinal pigmented epithelium cells. Furthermore, we demonstrate that ICRDS is insensitive to scattering effects using suspensions of copolymer microspheres and an absorbing dye solution. These results are compared with measurements made using a more traditional transmission-style setup. This technique will have an impact on the field of nanoscience, where optical characterization of nanoparticles is still done using a conventional spectrometer that is only capable of providing measurements of the extinction coefficient.

OCIS codes: (170.6510) Spectroscopy, tissue diagnostics; (300.1030) Absorption; (170.7050) Turbid media.

http://dx.doi.org/10.1364/OPTICA.2.000162

1. INTRODUCTION

Accurate knowledge of the absorption coefficient of biological cells and their constituents is of great importance in the fields of biology and medicine. Biomedical imaging techniques, modeling of light transport in tissue, and laser-based procedures such as laser refractive surgery all depend on these data [1–5]. That being said, much of the previous work in this area has relied on transmission-style experiments that measure attenuation, as opposed to absorption [6,7]. Biological tissues often produce strong scattering, so the measured attenuation (or extinction) may include a significant contribution from losses due to this scattering [8]. Thus, to find the absorption coefficient, these scattering losses must be either independently measured or numerically modeled.

Integrating cavities have been shown to be an exceptional tool for measuring low absorption coefficients, even when there is strong scattering in the sample [9–15]. The high diffuse reflectivity of the cavity walls allows for long effective optical path lengths through the sample medium. Additionally, the Lambertian behavior of the cavity wall leads to an isotropic field inside the cavity, eliminating the effects of scattering in the sample. More recently, integrating cavities have been used to enhance the detection of extremely low concentrations of biological waste products in water supplies [16].

O'Keefe and Deacon developed cavity ring-down spectroscopy (CRDS) as a technique for highly sensitive measurements of low absorption coefficients [17]. CRDS involves sending a temporally short laser pulse into a high-finesse two-mirrored cavity and observing the exponential decay, or "ring-down," of the intensity inside the cavity. While CRDS is a very powerful technique, it is inherently unable to distinguish losses due to absorption from losses due to scattering. Much like other transmission-style experiments, it is the attenuation that is being measured. This issue is clearly a substantial problem for samples that produce a large amount of scattering. Here, we employ integrating cavity ring-down spectroscopy (ICRDS) as a novel technique for measuring the optical absorption coefficient independent of scattering effects [14,15]. In ICRDS, the mirrored cavity used in traditional CRDS is replaced with a high-reflectivity integrating cavity. Traditional CRDS also requires that the input source is mode-matched to the mirrored cavity, and thus significant adjustments are needed in order to make measurements over a range of wavelengths [17,18]. Due to the diffuse nature of the light inside an integrating cavity, there are no preferred cavity modes. Therefore, ICRDS can be used over the entire range for which the wall reflectivity is sufficiently high, without any need for adjustments to the source or cavity [14,15]. To demonstrate the effectiveness of ICRDS, we have measured the absorption coefficient of retinal pigmented epithelium (RPE) cells.

2. METHODS

A. Integrating Cavity Ring-Down Spectroscopy

The diagram in Fig. 1 shows a cross-section of an ICRDS cavity. The diffuse reflecting walls of the cavity are made of a packed fumed silica, or quartz powder. This material has previously been shown to be an exceptional diffuse reflector in the UV and visible portions of the spectrum, with measured reflectivities as high as 0.9992 and 0.9969 at 532 and 266 nm, respectively [14,15]. A multimode fiber is used to deliver a temporally short laser pulse into the cavity. A second multimode fiber samples the exponential decay of the irradiance on the cavity wall. For an empty cavity, the decay constant τ for this exponential decay is given by the expression [14,15,19]

$$\tau = \frac{1}{-\ln \rho}\left(\frac{\bar{d}}{c} + \delta t\right). \quad (1)$$

Here, ρ is the cavity reflectivity, $\bar{d}$ is the average distance between the successive reflections in the cavity, and c is the speed of light. Fry *et al.* have previously shown that $\bar{d}$ can easily be calculated for a cavity of arbitrary geometry using only the cavity volume V and surface area S, via the expression $\bar{d} = 4(V/S)$ [19]. When photons strike a diffuse reflecting surface, like the packed fumed silica of the cavity walls, a small fraction will scatter directly back into the sample region but the majority will penetrate into the cavity wall. Those photons that penetrate into the surface will either reemerge into the sample region through multiple scattering or leave the cavity altogether. The δt term in Eq. (1) accounts for the average of this "wall-time" for each reflection [14,15].

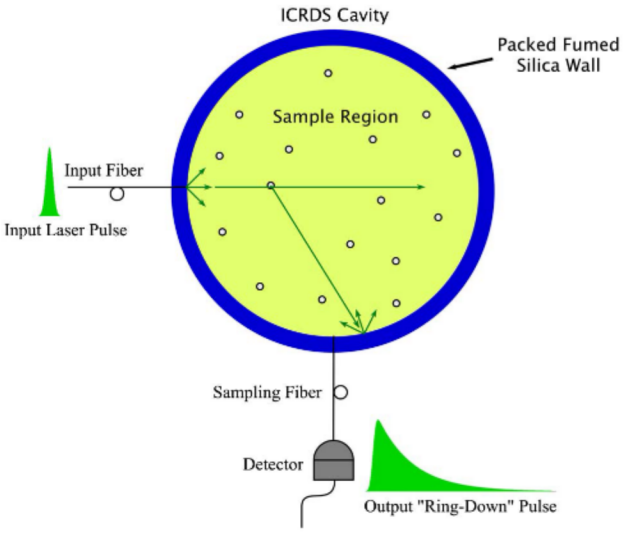

Fig. 1. Cross-section of an ICRDS cavity.

Figure 2 shows a typical ring-down decay curve for an empty cylindrical cavity with a diameter of 3.81 cm and height of 6.47 cm. The blue curve is the input laser pulse, the black curve is the output ring-down decay signal for the cavity, and the red curve is a fit to the decay curve. The fitting function used is the convolution of a Gaussian pulse and an exponential decay.

For the case when the cavity in Fig. 1 is filled with an absorbing sample, Eq. (1) becomes

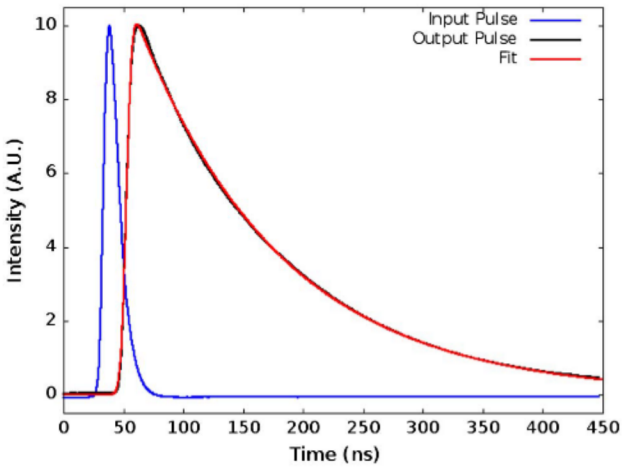

Fig. 2. Typical ring-down decay curve at 532 nm for an empty fumed silica cavity. The fit to the ring-down curve gives a decay constant of $\tau = 120.5$ ns, yielding a cavity reflectivity of 0.9992 [14,15].

$$\tau_s = \frac{1}{-\ln \rho + a_s \bar{d}} \left(\frac{\bar{d}}{c} + \delta t \right), \quad (2)$$

where a_s is the absorption coefficient of the sample and τ_s is the new cavity decay constant. It is clear from Eq. (2) that adding an absorbing sample will reduce the decay constant for the cavity. Therefore, if one measures the decay constant when the cavity is empty, as well as when the cavity contains the sample, then Eqs. (1) and (2) can be used to determine the absorption coefficient.

B. Sample Preparation

Human telomerase reverse transcriptase transformed human retinal pigmented epithelium cells (hTERT-RPE) *in vitro* were used for this work [20]. Cells were purchased from the American Type Culture Collection (ATCC, CRL-4000), and a detailed description of the culture methods has previously been published [21]. Briefly, the cells are grown using media composed of a 50:50 mix of DMEM:F12 supplemented with 10% (v:v) fetal bovine serum (Atlanta Biological), 10 mM HEPES (Fisher Scientific), 2 mM l-glutamine (Mediatech), 100 IU/ml penicillin (Mediatech), 100 μg/ml streptomycin, and 50 μg/ml gentamycin sulfate (Mediatech), hereafter referred to as complete medium (CM). Cells are grown in an incubator maintained at 37°C, 5% CO_2, and 100% relative humidity. Cell stocks are maintained in CM at subconfluence in T-75 flasks (BD or Corning) by splitting twice per week, either three or four days apart. Cells to be used for experiments are set from cell stocks at the time they are split. Transfers are split by removing the CM and rinsing the monolayer with 10 mL of Hanks Balanced Salt Solution (HBSS, Mediatech). The HBSS is then removed and replaced with 2 mL of 0.05% trypsin (Mediatech) with 0.53 mM ethylene diamine tetraacetate (EDTA, Mediatech) in HBSS. The flasks are returned to the incubator for 10 min with gentle agitation at the 5 min point. Cells are then removed from the incubator, 8 mL of CM is added to stop the action of the trypsin, and the resulting suspension is triturated 10 times to break up clumps and produce a single-cell suspension. Cells are then counted using a Coulter Counter (Beckman-Coulter) and appropriate numbers plated for future use. Cells to be used for experiments are either set into the specific tissue culture-ware format to be used for the experiment or into transitional plasticware, usually a 100 mm dish (P-100, BD or Corning), for later use. Under these conditions, the hTERT-RPE cells have a doubling time of ~21 h in exponential growth, and a single-cell colony-forming efficiency (plating efficiency) of ~40% when 20 to 80 cells are plated into a 35 mm dish (P-35, BD or Corning) with 3 mL of CM and allowed to grow undisturbed for 10 days. The data reported herein were obtained using exponentially growing cells.

C. Experimental Setup

The basic setup for the experiment is shown in Fig. 3(a). The laser source was a Quanta Ray Pro290 Nd:YAG-pumped VersaScan 355 midband OPO that produced a 6 ns pulse, and was tunable over a range of 412–2550 nm. To prevent detector saturation, the beam was attenuated with a filter wheel before being launched into the multimode fiber that was used to couple the input pulse into the integrating cavity. Another multimode fiber sampled the ring-down signal inside the cavity. This signal was sent to a Thorlabs DET 100 photodiode. An oscilloscope and LabVIEW VI were used to average (typically 50 shots) and record the data.

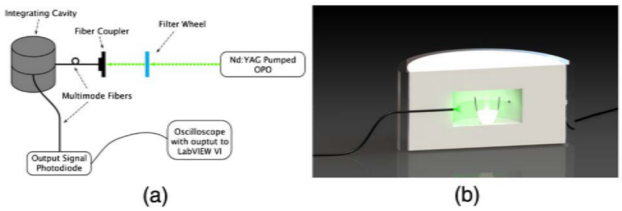

Fig. 3. Diagrams showing (a) the experimental setup for ICRDS absorption measurements and (b) a cross-section of the integrating cavity with the quartz crucible sample container.

Samples of the RPE cells were suspended in Dulbecco's phosphate buffered saline (PBS, Mediatech) solution during the ICRDS measurements. The overall sample size for the RPE cell solution was 3 mL, and contained 60 million cells. These samples were pipetted into a quartz crucible, which was then placed into a fumed-silica-integrating cavity [see Fig. 3(b)]. The integrating cavity we used had a cylindrical inner geometry with a 6.35 cm diameter and 6.35 cm height.

Clearly, the RPE cell sample (3 mL) occupies only a small portion of the inner cavity volume. This difference in volume requires the use of two samples of known absorption to calibrate the cavity. In addition to these calibration samples, a sample of the PBS solution must also be measured so that its contribution to the total absorption coefficient of the sample can be subtracted out.

If we consider Eq. (2) for the case of our RPE suspension, we have

$$\tau_{\mathrm{RPE}} = \frac{1}{-\ln \rho + (a_{\mathrm{PBS}} + a_{\mathrm{RPE}})\bar{d}_s} \left(\frac{\bar{d}}{c} + \frac{\bar{d}_s}{c_s} + \delta t \right), \quad (3)$$

where τ_{RPE} is the decay constant for the RPE suspension, $\bar{d}_s$ is the average distance between reflections in the sample, c_s is the speed of light in the sample, $\bar{d}$ is the average distance between reflections excluding the distance in the sample, c is the speed of light in air, and a_{PBS} and a_{RPE} are absorption coefficients for the PBS buffer and the RPE cells, respectively. Similarly, for a solution of pure water and dye, we have

$$\tau_D = \frac{1}{-\ln \rho + (a_{pw} + a_D)\bar{d}_s} \left(\frac{\bar{d}}{c} + \frac{\bar{d}_s}{c_{pw}} + \delta t \right), \quad (4)$$

where a_{pw} is the absorption coefficient of pure water, a_D is the absorption coefficient of the dye, and c_{pw} is the speed of light in pure water. Thus, if we measure the decay time for equal volumes of the RPE cell suspension, the PBS buffer, and two dye solutions, we can use Eqs. (3) and (4) to derive the following expression for the absorption coefficient of the RPE cells:

$$a_{\mathrm{RPE}} = \frac{\tau_{\mathrm{RPE}}^{-1} - \tau_{\mathrm{PBS}}^{-1}}{\tau_{D1}^{-1} - \tau_{D2}^{-1}}(a_{D1} - a_{D2}). \quad (5)$$

It should be noted that, in this derivation, it is assumed that $c_{pw} \approx c_{\mathrm{PBS}}$. Work by Diéguez *et al.* and Quan *et al.* show this to be a very reasonable assumption, with the percent difference between the index of refraction for PBS solution and water being less than 1% at 25°C [22,23]. The small size of this percent difference is not surprising, as the PBS buffer is simply a water-based isotonic solution.

A solution of ultrapure water and Irgalan Black, a water-soluble organic powder, served as the master dye for these experiments. The two dye solutions used in the measurements were prepared by diluting known amounts of this master dye with additional ultrapure water. The absorption coefficient of the master dye was determined separately using an Agilent Cary 6000i spectrophotometer, and these data were then used to calculate a_{D1} and a_{D2}.

3. RESULTS AND DISCUSSION

Figure 4 shows the results of ICRDS measurements of the absorption coefficient from 420 to 630 nm for a sample containing 60 million RPE cells suspended in PBS solution. The contribution to the absorption coefficient due to the buffer has been subtracted out. The data clearly show that the absorption coefficient for the cells drops by more than an order of magnitude as we shift across the visible spectrum toward the infrared.

Although the source allowed for tuning from roughly 412 to 2550 nm, several factors limited this initial study to the region from 420 to 630 nm. First, the output signal below 420 nm was too low to be used. This signal issue also occurred at 515 nm, so this data point was also excluded from Fig. 4. For the region above 630 nm, the absorption of water starts to dominate. The buffer used (PBS solution) is water based, and thus the majority of the volume of the sample is water. This effect was exacerbated by the fact that the absorption coefficient of the Irgalan Black calibrating dye drops off considerably beyond 650 nm. Additionally, we have found that the reflectivity of the fumed silica integrating cavities decreases as one moves into the infrared. Measurements at 1064 nm give cavity reflectivities of 0.995 (down from as high as 0.9992 at 532 nm). While these factors combined to reduce the wavelength range for this initial work, there are several simple steps that can be taken to expand the range of future experiments. These steps are discussed in the conclusion.

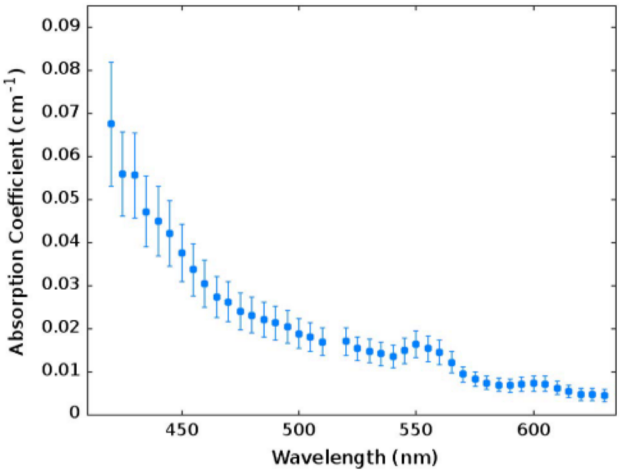

Fig. 4. ICRDS measurements of the absorption coefficient from 420 to 630 nm for a sample containing 60 million RPE cells suspended in PBS solution (the total volume of the cell/PBS solution was 3 mL). The contribution to the absorption coefficient due to the buffer solution has been subtracted out. Due to low output signal, the data point at 515 nm has been excluded.

The error bars shown in Fig. 4 result from a combination of the uncertainty in the decay constants, the accuracy of the concentration of the calibrating dye solutions, and the accuracy of the spectrophotometer used to measure the absorption coefficient of the master dye solution. Previous work with the fumed silica integrating cavities has demonstrated a relative uncertainty of 1% for the measured empty cavity decay constant [15]. However, this can increase slightly as the decay constant decreases due to the presence of an absorber. For this reason, we have used a fixed uncertainty of ±1.5 ns for all of the measured decay constants (i.e., $\delta\tau_{\mathrm{RPE}}$, $\delta\tau_{\mathrm{PBS}}$, $\delta\tau_{D1}$, and $\delta\tau_{D2}$). This gives a relative uncertainty of ∼1% for the highest decay constants and ∼5% for the lowest. These uncertainties are then propagated in accordance with Eq. (5) for each wavelength. The calibrating dye solutions were prepared by pipetting small amounts (7 mL ±1% for dye 1, and 5 mL ±1% for dye 2) of the master dye solution, and then diluting with ultrapure water to a volume of 250 mL ±0.05% in a volumetric flask. An Agilent Cary 6000i spectrophotometer, with a photometric accuracy of 0.0003 absorbance units, was used to measure the absorption coefficient of the master dye solution. The resulting relative uncertainties were less than 20% for the data from 420 to 580 nm, less than 22% from 585 to 605 nm, and less than 28% from 610 to 630 nm.

We can gain some insight into the advantages of this new ICRDS technique by comparing these results with a transmission-style measurement. To make this comparison, we took the same sample of RPE cells and pipetted them into a 10 mm × 10 mm quartz cuvette. We then used an Agilent Cary 6000i spectrophotometer to measure the absorbance of the cell sample. A blank of the PBS buffer solution was also measured and subtracted out. Figure 5 shows the results of the spectrophotometer measurements, along with the ICRDS data for the same sample. The ICRDS data clearly show a structure that is not seen in the spectrophotometer data. Additionally, the spectrophotometer data give values that are on average ∼100 times larger than the ICRDS values (note the two vertical scales in Fig. 5). This difference is entirely due to the large losses from scattering in the RPE cell sample. In other words, the spectrophotometer is measuring the attenuation coefficient for the sample, whereas ICRDS is providing a true measurement of the absorption coefficient.

Furthermore, we performed a simple test to verify that the ICRDS technique is insensitive to scattering in the sample. This test involved measuring the decay constants for sample suspensions of scattering particles with increasing concentration. The scatterers used were transparent Duke Scientific

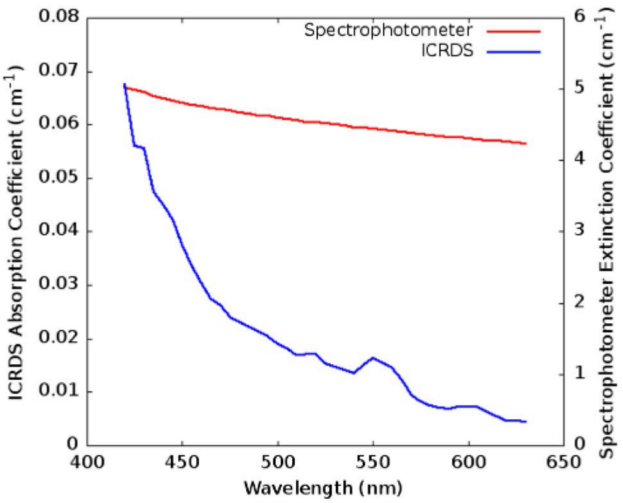

Fig. 5. Comparison of ICRDS and spectrophotometer measurements for the absorption coefficient of RPE cells. The left vertical scale corresponds to the ICRDS data, while the right vertical scale corresponds to the spectrophotometer data.

copolymer microspheres in a 10% w/w water suspension (catalog no. 7508). The microspheres had a mean diameter of 8 μm. Small volumes (1, 3, and 5 mL) of this master suspension were diluted with ultrapure water to a volume of 500 mL to make three sample suspensions. Three additional samples were prepared using a dilution of the same Irgalan Black master dye used in the ICRDS measurements. The first of these contained only the master dye diluted by a factor of 100 with pure water. The other two samples used the same diluted dye, but also included a small volume of the master scatterer suspension (1 and 2 mL of scatterers added, respectively).

The ring-down decay constant for a 5 mL sample of each of these suspensions was measured using the 532 nm output of a Continuum Powerlite Precision 9010 Nd:YAG laser (10 ns pulse), and a Hamamatsu 1P21 PMT for detection. The basic setup was essentially the same as that shown in Fig. 3. Table 1 shows the results of these ring-down measurements. The decay constants for the three scattering suspensions remained nearly identical, despite the fivefold increase in scatterer concentration. The small differences seen (less than 1.5%) are well within the relative uncertainty of the absorption measurements just shown. The addition of the absorbing dye to the solution drops the decay constant from 133.0 to 89.1 ns. However, the addition of scatterers to this dye solution produces almost no change to measured decay constant. Again the differences between the various samples were all less than 1.5%.

Table 1. Ring-Down Decay Constants for Suspensions of 8 μm Scatterers with Increasing Concentration, and for Suspensions of an Absorbing Dye Solution and Scatterers

Sample (all sample volumes are 5 mL)	Decay Constant (ns)
Scatterers (1 mL diluted to 500 mL)	133.5
Scatterers (3 mL diluted to 500 mL)	131.5
Scatterers (5 mL diluted to 500 mL)	133.0
Dye solution (no scatterers)	89.1
Dye solution + 1 mL scatterers	89.1
Dye solution + 2 mL scatterers	87.8

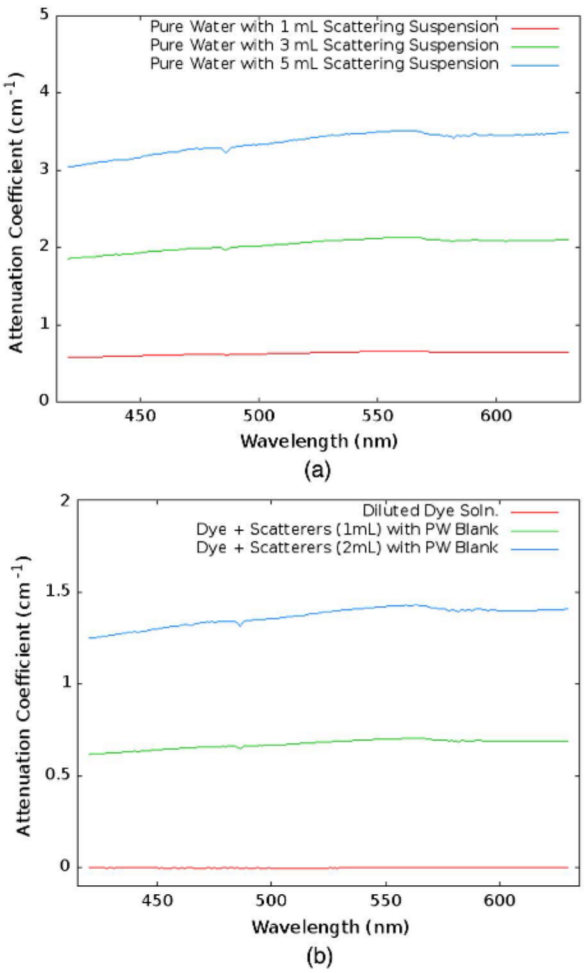

Fig. 6. Spectrophotometer measurements of (a) the attenuation coefficient for suspensions of pure water and 8 μm copolymer microsphere scatterers and (b) the attenuation coefficient for dye solutions with and without scatterers.

We also measured the same set of samples with an Agilent 8453 UV–VIS spectrophotometer. Figures 6(a) and 6(b) show the results from these measurements. For the scatterer suspensions [Fig. 6(a)], we see that the measured attenuation (or extinction) coefficient increases proportionally with the increased concentration of scatterers in the sample. For the dye samples [Fig. 6(b)], we once again see a nearly proportional increase in the measured attenuation coefficient with increasing scatterer concentration. In fact, the spectrophotometer gives negative values over much of the visible spectrum for the dye solution without scatterers (the light blue curve), indicating that the dye solution is below the detection threshold for the instrument. Comparison of the various plots in Figs. 6(a) and 6(b) shows that the scatterers actually dominate the signal, and are responsible for nearly all the measured attenuation for the dye/scatterer solutions.

In order to investigate the effects of smaller scatterers, a second test was performed using suspensions of 1 μm latex

Table 2. Ring-Down Decay Constants for Suspensions of an Absorbing Dye Solution and 1 μm Scatterers with Increasing Concentration

Sample (all sample volumes are 5 mL)	Decay Constant (ns)
Dye solution (no scatterers)	90.4
Dye solution + 0.250 mL scatterers	89.9
Dye solution + 0.500 mL scatterers	90.8
Dye solution + 0.750 mL scatterers	90.7
Dye solution + 1.000 mL scatterers	93.8
Dye solution + 1.250 mL scatterers	94.0
Dye solution + 1.500 mL scatterers	95.6

microspheres (Thermo Scientific Latex Microsphere Suspension, 10% w/w water suspension, catalog no. 5100A). As in the previous test, a 500 mL solution of the diluted Irgalan Black master dye (125× dilution) was prepared, and the decay constant for a 5 mL sample was measured. Then, small volumes (0.250 mL at a time) of the master scattering suspension (10% w/w water suspension) were added to the dye solution and decay constants were measured at 532 nm for 5 mL samples at each concentration. Table 2 shows the results from these measurements. It is clear that there is no significant effect from the presence of the scatterers until a total of 1 mL of the scattering suspension has been added. At this point, there is a 3.7% difference between the decay constant of the suspension and the decay constant of the dye solution with no scatterers. For the three concentrations below this, the percent difference is less than 1% and within the expected uncertainty of the decay constant. Like the previous test, the various samples were taken to a spectrophotometer in order to determine the attenuation coefficient for each suspension. Only the first two scattering suspensions could be measured in this way, as the higher-concentration samples were too strongly attenuating for the spectrophotometer being used (Agilent 8453). Thus, the data from the two lowest-concentration samples was used to extrapolate the attenuation coefficients for the higher-concentration samples. Based on this, the attenuation coefficients for the suspensions with 0.750 and 1.000 mL of scatterers were ∼9 cm^{-1} and ∼12 cm^{-1}, respectively. It should be noted that these attenuation values are more than 1000 times higher than the measured absorption coefficient (0.0043 cm^{-1}) of the dilute dye solution used for these tests.

As a final test, we prepared a second dye solution to act as an unknown absorber. This unknown was a dilute solution of Alcian Blue powder and ultrapure water. In addition, three dilutions (50×, 38.46×, and 31.25×) of the Irgalan Black master dye were prepared to act as the calibrating solutions for the measurement. Ring-down tests were performed at 532 nm for 5 mL samples of all four dyes and a 5 mL sample of pure water. Additionally, a sample of the Irgalan Black master dye was measured in an Agilent 8453 spectrophotometer. The decay constants for the various samples, as well as the absorption data from the spectrophotometer, were then used to calculate the absorption coefficient of the unknown Alcian Blue dye via Eq. (5). This was then compared to the absorption coefficient obtained by measuring a more concentrated (125×) solution of the Alcian Blue dye in the spectrophotometer. When the two highest-dilution calibrating dyes were used, the percent difference between the ICRDS measurement and the spectrophotometer measurement was only 2.7%. However, when the highest- and lowest-dilution calibrating dyes were used, then this percent difference was 11.8%. Finally, if the two lowest-dilution calibrating dyes were used, the percent difference was 21.7%. This data suggests that higher-dilution (i.e., lower-concentration) dyes are best for calibrating the ICRDS measurements. For the RPE cell measurements just presented, the two calibrating dyes had dilution factors of 50× and 35.71× for the same master dye solution. Thus, the error bars given for the RPE cell data appear to be adequate.

These results demonstrate the critical importance that scattering plays when making absorption measurements with a transmission-style experiment. ICRDS shows a clear ability to directly measure small absorption coefficients, while simultaneously being insensitive to the effects of scattering in the sample.

4. CONCLUSIONS

We have demonstrated that ICRDS provides a highly sensitive technique for measuring the absorption coefficient of low-absorbing samples, even in the presence of strong scattering. We also compared the results of ICRDS with spectrophotometer data to demonstrate the need for direct measurements of the absorption coefficient, as opposed to the attenuation coefficient, which is the quantity measured with transmission-style experiments. It should be noted that for this work the sample size was extremely small (3 mL total volume), and that larger sample sizes should allow for reduced uncertainty in the measurements. The wavelength range of the measurements could be expanded with some basic adjustments. For instance, using a stronger absorbing dye above 630 nm would allow for better discrimination between the absorption due to sample and the absorption due to the water in the buffer solution, and thus allow the measurements to be extended further toward the infrared. Increasing the cell-to-buffer ratio could provide a similar benefit. The integrating cavity itself can also be modified. While the fumed silica powder is an exceptional choice for the ICRDS diffuse reflector in the UV and visible, there is no reason that another material could not be used for other portions of the spectrum. As a final comment, while this work centered on measuring the absorption coefficient for cells suspended in liquid solutions, this technique could also be used to look at absorption in bulk tissue, subcellular constituents, aerosolized particles, or even trace gases.

FUNDING INFORMATION

George P. Mitchell Chair in Experimental Physics; National Science Foundation (NSF) (CBET-1250363, DBI-1250361, ECCS-1250360); Office of the Chief Scientist, 711 Human Performance Wing and the Optical Radiation Bioeffects Branch of the USAF Research Laboratory; Robert A. Welch Foundation (A-1218). Research performed by TASC, Inc. was conducted under USAF Contract (FA8650-08-D-6930).

REFERENCES

1. S. Flock, M. Patterson, B. Wilson, and D. Wyman, "Monte Carlo modeling of light propagation in highly scattering tissues. i. model predictions and comparison with diffusion theory," IEEE Trans. Biomed. Eng. **36**, 1162–1168 (1989).
2. C. R. Munnerlyn, S. J. Koons, and J. Marshall, "Photorefractive keratectomy: a technique for laser refractive surgery," J. Cataract Refract. Surg. **14**, 46–52 (1988).
3. M. Loughnan, "Laser refractive surgery," Aust. Family Physician **27**, 154–158 (1998).
4. K. Muellner, E. Bodner, G. E. Mannor, G. Wolf, T. Hofmann, and W. Luxenberger, "Endolacrimal laser assisted lacrimal surgery," British J. Ophthalmol. **84**, 16–18 (2000).
5. W.-F. Cheong, S. Prahl, and A. Welch, "A review of the optical properties of biological tissues," IEEE J. Quantum Electron. **26**, 2166–2185 (1990).
6. J. C. Murchio and M. B. Allen, "Measurement of absorption spectra of chlorophyll in algal cell suspensions," Photochem. Photobiol. **1**, 259–266 (1962).
7. J. R. Mourant, R. R. Gibson, T. M. Johnson, S. Carpenter, K. W. Short, Y. R. Yamada, and J. P. Freyer, "Methods for measuring the infrared spectra of biological cells," Phys. Med. Biol. **48**, 243–257 (2003).
8. J. R. Mourant, J. P. Freyer, A. H. Hielscher, A. A. Eick, D. Shen, and T. M. Johnson, "Mechanisms of light scattering from biological cells relevant to noninvasive optical-tissue diagnostics," Appl. Opt. **37**, 3586–3593 (1998).
9. P. Elterman, "Integrating cavity spectroscopy," Appl. Opt. **9**, 2140–2142 (1970).
10. E. S. Fry, G. W. Kattawar, and R. M. Pope, "Integrating cavity absorption meter," Appl. Opt. **31**, 2055–2065 (1992).
11. R. M. Pope and E. S. Fry, "Absorption spectrum (380–700 nm) of pure water. ii. Integrating cavity measurements," Appl. Opt. **36**, 8710–8723 (1997).
12. D. J. Gray, G. W. Kattawar, and E. S. Fry, "Design and analysis of a flow-through integrating cavity absorption meter," Appl. Opt. **45**, 8990–8998 (2006).
13. J. A. Musser, E. S. Fry, and D. J. Gray, "Flow-through integrating cavity absorption meter: experimental results," Appl. Opt. **48**, 3596–3602 (2009).
14. M. T. Cone, "A new diffuse reflecting material with applications including integrating cavity ring-down spectrscopy," Ph.D. thesis (Texas A&M Universtiy, 2014).
15. M. T. Cone, J. A. Musser, E. Figueroa, J. D. Mason, and E. S. Fry, "Diffuse reflecting material for integrating cavity spectroscopy—including ring-rown spectroscopy," Appl. Opt. **54**, 334–346 (2015).
16. J. N. Bixler, M. T. Cone, B. H. Hokr, J. D. Mason, E. Figueroa, E. S. Fry, V. V. Yakovlev, and M. O. Scully, "Ultrasensitive detection of waste products in water using fluorescence emission cavity-enhanced spectroscopy," Proc. Natl. Acad. Sci. USA **111**, 7208–7211 (2014).
17. A. O'Keefe and D. A. G. Deacon, "Cavity ring-down optical spectrometer for absorption measurements using pulsed laser sources," Rev. Sci. Instrum. **59**, 2544–2551 (1988).
18. P. Zalicki and R. N. Zare, "Cavity ring-down spectroscopy for quantitative absorption measurements," J. Chem. Phys. **102**, 2708–2717 (1995).
19. E. S. Fry, J. Musser, G. W. Kattawar, and P.-W. Zhai, "Integrating cavities: temporal response," Appl. Opt. **45**, 9053–9065 (2006).
20. A. G. Bodnar, M. Ouellette, M. Frolkis, S. E. Holt, C.-P. Chiu, G. B. Morin, C. B. Harley, J. W. Shay, S. Lichtsteiner, and W. E. Wright, "Extension of life-span by introduction of telomerase into normal human cells," Science **279**, 349–352 (1998).
21. M. L. Denton, M. S. Foltz, L. E. Estlack, D. J. Stolarski, G. D. Noojin, R. J. Thomas, D. Eikum, and B. A. Rockwell, "Damage thresholds for exposure to NIR and blue lasers in an in vitro RPE cell system," Investig. Ophthalmol. Vis. Sci. **47**, 3065–3073 (2006).
22. L. Diéguez, N. Darwish, M. Mir, E. Martínez, M. Moreno, and J. Samitier, "Effect of the refractive index of buffer solutions in evanescent optical biosensors," Sens. Lett. **7**, 851–855 (2009).
23. X. Quan and E. S. Fry, "Empirical equation for the index of refraction of seawater," Appl. Opt. **34**, 3477–3480 (1995).